

## General Disclaimer

### One or more of the Following Statements may affect this Document

- This document has been reproduced from the best copy furnished by the organizational source. It is being released in the interest of making available as much information as possible.
- This document may contain data, which exceeds the sheet parameters. It was furnished in this condition by the organizational source and is the best copy available.
- This document may contain tone-on-tone or color graphs, charts and/or pictures, which have been reproduced in black and white.
- This document is paginated as submitted by the original source.
- Portions of this document are not fully legible due to the historical nature of some of the material. However, it is the best reproduction available from the original submission.

NASA CR-

151724

A NOTE ON THE TISSUE STAR DOSE  
IN PERSONNEL RADIATION MONITORING IN SPACE

Hermann J. Schaefer

(NASA-CR-151724) A NOTE ON THE TISSUE STAR  
DOSE IN PERSONNEL RADIATION MONITORING IN  
SPACE (West Florida Univ., Pensacola.) 17 p  
HC A02/MF A01

CSSL C6F

N78-25758

Unclas

G3/52 21617



April 1978

Faculty of Physics  
The University of West Florida  
Pensacola, Florida 32504



A NOTE ON THE TISSUE STAR DOSE  
IN PERSONNEL RADIATION MONITORING IN SPACE

Hermann J. Schaefer

National Aeronautics and Space Administration  
Contract NAS 9-15417

Approved by

Alfred B. Chaet  
Associate Vice President for  
Research and Sponsored Programs

Released by

James A. Robinson  
President  
The University of West Florida

15 April 1978

Faculty of Physics  
The University of West Florida  
Pensacola, Florida 32504

## SUMMARY

### THE PROBLEM

Secondaries from nuclear interactions of high-energy primaries in the body tissues themselves contribute substantially to the astronaut's radiation exposure in space. The so-called tissue star dose is assessed from the prong number distribution of disintegration stars in emulsion. Separating the tissue-equivalent gelatin stars from the silverbromide stars requires prong-counting a large number of stars for statistical accuracy. For operational use of the method on Space Shuttle flights, minimum scanning time requirements have to be closely determined.

### FINDINGS

Prong counts of 1,000 emulsion stars from the Apollo-Soyuz mission reported earlier were re-evaluated. The original scores were divided into sets of 250, 500, 750, and 1,000 emulsion stars and the respective prong number distributions established. The statistical error of the gelatin star number for the four consecutively larger sets was found to vary, on the 67 percent confidence level, from  $\pm 25$  percent for the count of 250 emulsion stars to  $\pm 11$  percent for 1,000 stars. Seen in the context of the other limitations of the experimental design, the lowest effort of prong-counting 250 stars appears entirely appropriate. Further substantial savings in scanning manhours could be accomplished by forgoing the prong count completely and establishing the gelatin star number as a constant fraction of the total count based on the star ratios determined with the full method on earlier missions.

## INTRODUCTION

A very elusive part of the astronaut's radiation exposure in space is produced by secondaries from nuclear interactions in the body tissues themselves. Depending on the energy of the primary particle initiating the nuclear collision, the types and energies of the secondaries can vary widely. However, by far the most frequent kind of interaction is the evaporation star, commonly called tissue disintegration star when dosimetric implications are discussed. A star represents a simultaneous burst of several neutrons, protons, and alpha particles of comparatively low energies. Accordingly, it is a strictly local event with maximum ranges of the secondaries in tissue centering heavily on values well below 1 millimeter. At the same time, the Linear Energy Transfer (LET) spectrum of the secondaries is such that Quality Factors (QF's) greatly exceeding 1.0 have to be applied for establishing dose equivalents.

The effect of secondaries of short range from tissue stars on the local dose becomes conspicuously apparent when the depth dose distribution of a monoenergetic beam of high-energy protons entering a tissue-equivalent phantom from vacuum or air is measured with sufficiently small sensors. Figure 1 based on data reported by Tanner, Baily, and Hilbert (1) shows the initial section of such a distribution. The authors used a parallel beam of 730 Mev protons with a cross section of 12 x 12 inches entering a polystyrene phantom. An all-polystyrene design with a very thin air sheet as ion chamber provided complete tissue-equivalent homogeneity and millimeter accuracy in resolving depth along the beam. The steep, rapidly saturating increase of the local dose in the initial few tenths millimeter strikingly indicates that secondaries of very short range must be responsible for the build-up. It should be noted that the effect can not be demonstrated with proton radiation in space because of the omnidirectional incidence and the complex shield distribution about any measuring device carried in a space vehicle. It should be noted furthermore that Figure 1 shows the radiation level in relative units of absorbed dose. The high QF values mentioned above for the low-energy protons and alpha particles involved in the build-up substantially enhance the effect in terms of the dose equivalent.

As seen from the quoted reference, the measurement of the absorbed dose along the beam in the phantom already requires highly sophisticated instrumentation. Even more formidable difficulties arise if one sets out to determine local dose equivalents, i.e., resolve the LET spectrum. In fact, no simple reliable method exists which would be acceptable for operational use and still meet minimum requirements for accuracy. On manned missions of the past, the tissue star dose has either been disregarded completely or only determined semi-quantitatively by indirect methods. In a preceding report, hereafter referred to as Report 2, such a method has been described in its application to nuclear emulsion data from the Apollo-Soyuz mission.

As Report 2 amply demonstrates, the large effort of prong-counting 1,000 emulsion stars contrasts with the rather modest result of a semi-quantitative estimate of the tissue star dose. Nevertheless, as no other method seems available at this time, a systematic study of the capabilities and limitations of the emulsion method for assessing the tissue star dose appears of interest. The present report continues the earlier study and examines in more detail the shortcomings of emulsion as an essentially two-dimensional medium and the relationships governing the statistical accuracy of the final result. The latter problem is of special importance because the net count of emulsion stars evolves from the gross count of all stars by a complex method. Specific data on the compound error are essential for a realistic appraisal of the counting time requirements.

#### STAR RECORDING EFFICIENCY OF EMULSION

As mentioned before, the bulk of the tissue star dose accrues from evaporation stars, i.e., from stars producing secondaries of comparatively low energies in the interval from a few to some 30 Mev. Figure 1 in Report 2 has shown the energy spectra for star-produced neutrons, protons, and alpha particles. Converting energy to range in emulsion, we arrive at the range spectra for protons and alpha particles of Figure 3 of the present report. It is seen that particle fluences center heavily on the interval from 80 to several hundred micron emulsion. Comparing these ranges with the emulsion thickness of 100 microns most commonly used in space radiation dosimeters,

one realizes that only a certain fraction of the secondaries from evaporation stars, which are emitted essentially in all directions, will be completely contained within the emulsion layer. We proceed to examine the limitation in question in quantitative terms.

Assuming a fictitious star which would emit secondaries of strictly one range only with the star center located at depth  $x$  in the emulsion layer, we see from Figure 2 that the probability  $p$  for a randomly emitted particle to end in the emulsion is directly proportional to the fractional surface of the sphere of radius  $R$  which falls within the emulsion layer, where  $R$  stand for the range of the emitted particle. The complementary probability  $1 - p$  for a particle to leave the emulsion is proportional to the remaining surface of the sphere outside the emulsion. Analytically, the two probabilities expressed in terms of  $x$  and  $R$  are defined by the equations  $p = 2\pi(R + x)/4\pi R^2$  and  $1 - p = 2\pi(R - x)/4\pi R^2$ . Since the central plane within the emulsion is a plane of symmetry for the star prong geometry, it is advantageous to introduce half the emulsion thickness  $H = \frac{1}{2} D$  and express the particle range  $R$  as fraction  $f$  of  $H$  according to  $R = fH = \frac{1}{2}fD$ . A summation over the depth interval from  $x = 0$  to  $x = H$  furnishes the mean probability  $p_m$  for star prongs of range  $R$  originating at any depth to end within the emulsion layer. We call  $p_m$  the recording efficiency of an emulsion layer of thickness  $2H$ . An easy derivation shows that, for the interval  $0 \leq R \leq 2H$ , the efficiency obeys the relation  $p_m = 1 - f/4$  and, for ranges  $R \geq 2H$ , the relation  $p_m = 1/f$ .

The lower graph in Figure 3 shows the recording efficiency  $p_m$  as a function of  $R$  for the two emulsion thicknesses of 100 and 200 microns. Projecting the efficiency factors upon the range spectra in the upper graph, we see that the efficiency varies considerably depending on emulsion thickness and particle type. Multiplying instantaneous efficiencies with their respective particle frequencies, integrating, and taking the mean, we obtain the grand total recording efficiency for a given emulsion thickness. For the data of Figure 3 the indicated evaluation leads, for 100 micron emulsion, to grand totals of 5 percent for protons and 36 percent for alpha particles. For 200 micron emulsion, the corresponding values are 10

and 60 percent. Establishing the complete range spectra experimentally by star prong measurements is seen from these relationships to constitute an extremely tedious task requiring the examination of truly enormous numbers of stars.

A systematic exploitation of star populations in emulsions exposed to cosmic radiation has been carried out by Harding, Lattimore, and Perkins (3) long before the dawn of the space age, but has never been attempted on manned space missions. Instead, one has satisfied oneself with estimates of the star dose obtained by the theoretical spectra of Figure 3. The fraction of stars originating in the gelatin matrix of the emulsion, which represent the tissue-equivalent fraction of the total population, is established in such assessments from the prong number distribution of the total population. Since this approach utilizes all prongs, those ending within the emulsion as well as those leaving it, data acquisition in the scanning process is much faster. Yet even so, ensuring statistical significance of the gelatin star count requires a major scanning effort. However, since the method appears, at the present time, the only acceptable approach to operational radiation monitoring of the star dose, it seems of timely interest to examine the statistical aspects more closely.

#### STATISTICAL ACCURACY OF THE PRONG NUMBER METHOD

The basic steps in determining the net number of gelatin stars from the prong number distribution of the total star population in emulsion have been outlined in Report 2. For the reader's convenience, Figure 2 of the earlier study is shown again in Figure 4. The small circles denote integral star frequencies as they follow from the raw scores of the scanning procedure. It is seen that the data points strongly suggest, in a semilog plot, two straight lines as curves of best fit, one covering the prong number interval from 2 to 6 and the other the remaining higher prong numbers. Establishing the straight lines by the method of least squares and extrapolating the one for high prong numbers down to 2 prongs, one obtains the number of gelatin stars as the difference between the two lines as indicated in Figure 4 by the shaded area. Since gelatin can be considered a tissue-equivalent material, the energy deposited by the



gelatin stars directly defines the tissue star dose.

In Report 2, the just indicated evaluation has been based, in a straightforward way, on the prong number distribution of the total population of 1,000 scanned emulsion stars. In order to establish specific clues on the statistical variation of the net number of gelatin stars and its dependence on the total count, we now divide the original scores into four equal subsets of 250 stars each, re-assemble them to four new sets of 250, 500, 750, and 1,000 stars, and conduct separate evaluations of the net count of gelatin stars for each set. The evaluation of the 1,000 star set is, of course, identical to the earlier one presented in Report 2.

Table I shows the individual star numbers in the prong number classes for the four subsets of 250 stars each. That means the grand total of all entries equals 1,000 as is easily verified. For establishing the straight line of best fit, we lump together the classes of prong numbers 8 and 9, 10 and 11, and 12 and higher into three larger classes in order to ensure equal numbers of experimental points defining either line. Table II shows the system of adjusted prong number classes and the respective integral star numbers for the four sets obtained by cumulative additions of the entries in Table I.

Deriving the equations for the straight lines of best fit is a routine procedure. Tables I and II contain all input data for the calculation. We restrict explicit presentation to one example selecting the case of 500 stars. Calling the integral star number  $S$  (ordinate in Figure 4) and the prong number  $N$  (abscissa in same Figure) and remembering that the ordinate scale is linear in  $\log S$  and that the abscissa scale starts with 2 prongs, we can write the equation for the line of best fit in the general form  $\log S = a - b(N - 2)$  where two pairs of values  $a, b$  have to be calculated defining the two straight lines of best fit for the two sets of five experimental pairs of values  $S, N$  each. For the 500 set of Table II, we obtain the two equations

$$\begin{aligned}\log S &= 2.702 - 0.137(N - 2) \\ \log S &= 2.489 - 0.086(N - 2)\end{aligned}$$

for the low and high prong number intervals, respectively. Extrapolating the second equation to  $N = 2$ , we obtain  $\log S = 2.489$  or

$S = 308.3$  for the number of silverbromide stars. The first equation furnishes, for  $N = 2$ ,  $\log S = 2.702$  or  $S = 503.5$  for the total number of emulsion stars (silverbromide plus gelatin). The difference,  $503.5 - 308.3 = 195.2$ , represents the gelatin stars.

It is essential to realize that the final result of the foregoing evaluation, the number of gelatin stars, is obtained as the difference of two much larger numbers, namely, the one of all emulsion stars and the one of the silverbromide stars. Both numbers represent frequencies of random events. It is seen, then, that the system closely resembles the well known situation in the low-level assay of radioactive samples when an aliquot to be measured furnishes a smaller count than the background. Two counts have to be conducted in such cases, one of the background only and a second one of background plus sample. For the emulsion system, the Number of all emulsion stars is the counterpart to the sample-plus-background count and the number  $B$  of the silverbromide stars stands for the background count without the sample. According to the laws of statistics, the standard deviation  $s$  of the difference, i.e., the number of gelatin stars  $G = E - B$  is obtained as  $s = \sqrt{E + B}$ . The standard deviation  $s$  determines the statistical variation of  $G$ , usually written as  $G \pm s$ , on the 67 percent confidence level.  $1.96 s$  and  $2.58 s$  define the variation for the 95 and 99 percent confidence levels, respectively. Applied to the case of 500 counted emulsion stars, the evaluation furnishes, for the three confidence levels, gelatin star frequencies of  $195 \pm 28.5$  and  $195 \pm 56$  and  $195 \pm 73.5$ . Table III shows the values for all four star counts. We see, for the 67 percent confidence level, the accuracy improve from 24.5 percent for the count of 250 stars to  $\pm 11$  percent for 1,000 stars.

### CONCLUSIONS

Examining the findings from the viewpoint of operational radiation monitoring, we are mainly interested in the time economy of the scanning procedure. A reliable star prong count requires two runs, a first one at medium power locating the stars and a second one at high power prong-counting them. Depending on the density of the star population in the emulsion, a trained observer needs about 15 to 20 net scanning hours at the microscope for the prong count of 250

emulsion stars. This represents an unusually large expenditure of time for just one dose value. It compares very unfavorably to the time requirements for one reading in densitometric or solid state dosimetry. We are inclined, then, to settle for the lowest effort of prong-counting 250 stars. The corresponding rather large statistical error of  $\pm 25$  percent has to be judged in the context of all errors inherent in the experimental design. Obviously, if these other sources of errors already lower the accuracy to the  $\pm 25$  percent level, it would be useless to assess a star count with a substantially smaller statistical error.

The additional error sources in question are not only of normal experimental nature resulting from imperfections of the recording medium and observational deficiencies. More important is the uncertainty due to the fact that the method of approximating the prong number spectrum by two straight lines of different slope is essentially an empirical finding lacking a firm theoretical foundation in its quantitative aspects. The intranuclear dynamics of the evaporation process is not understood so well that one could predict the exact prong number distribution for different Z species of evaporating nuclei. While Z certainly defines the maximum possible number of fragments, any smaller number can also occur in processes of incomplete evaporation.

On the other hand, it is a strong argument in favor of the emulsion method that the breakdown of the total star population into silverbromide and gelatin stars as it follows from the change of slope of the prong spectrum agrees well with the interaction cross sections and abundances of the two components of emulsion. Other aspects, again, are less reassuring, especially those mentioned before concerning a full resolution of the energy spectrum of the secondaries. The determination of the tissue star dose from the theoretical spectrum is bound to further enhance the compound error of the method.

With all these uncertainties involved, the assessment of the tissue star dose from the prong number distribution qualifies only as a semi-quantitative method. Therefore, satisfying oneself with a low star count in the interest of time economy seems a reasonable approach. In fact, since the scanning effort is still comparably large

even for 250 stars, one might want to go further and settle for a still smaller number of counted stars. In this respect, the method could be modified and further simplified by establishing the gelatin star number directly as a fraction of the total star number utilizing the ratio of the two kinds as it follows from earlier measurements. For instance, the count of 1,000 emulsion stars on Apollo-Soyuz has furnished, according to Table III, a gelatin star number of 369. Comparing this number to the adjusted total star count of 1,006 as it follows from the equation of the line of best fit, we obtain a ratio of 0.367. Rounding off, we could use 0.35 as a constant factor for deriving the gelatin star number for all future missions directly from the total star count. In doing so, we would gain substantial savings in scanning manhours because the time-consuming prong count would no longer be needed.

As spelled out in Report 2, the emulsion method has furnished, for Apollo-Soyuz, a tissue star dose from protons and alpha particles of 7.8 millirad or 45 millirem with an additional 4.5 millirad or 45 millirem from star-produced neutrons. The resulting mean QF of 7.3 for the star dose demonstrates poignantly that we are dealing with high-LET radiation. That means good radiation safety practice makes it mandatory to record absorbed dose and LET spectrum. It seems strange that a contribution as substantial as the tissue star dose should have been treated as an insignificant entity for so long. To be sure, cosmic ray investigators became aware of the star phenomenon long before the space age. Harding, Lattimore, and Perkins (1.c., 3) published the first study of the capabilities and limitations of nuclear emulsion for star analysis in 1949 yet did not consider the role of the gelatin matrix. Birnbaum and Shapiro (4) were the first ones to observe the change of slope in the integral prong number distribution and interpret it as caused by the gelatin stars. Yagoda and Haymaker (5) pointed out the dosimetric implications. Development stopped at that point and the experimental technique has remained essentially unchanged ever since. As a consequence, we are faced now with the difficult task of adapting a tedious and complex laboratory procedure to routine personnel radiation monitoring on Space Shuttle flights. Nevertheless, one should not lose sight of the fact that

nuclear emulsion still provides by far the most complete record of the astronaut's radiation exposure among all available dosimetric systems. Properly processed, emulsion represents a permanent record allowing repeated read-outs by independent observers even after years when new evaluation techniques might be available.

#### REFERENCES

1. Tanner, R. L., Baily, N. A., and Hilbert, J. W., High-energy proton depth-dose patterns. Rad. Res. 32, 861 - 874, 1967.
  2. Schaefer, H. J., Nuclear emulsion measurements of the dose contribution from tissue disintegration stars on the Apollo-Soyuz mission. Faculty of Physics, University of West Florida, Pensacola, Florida 1977.
  3. Harding, J. B., Lattimore, S., and Perkins, D. M., Nuclear disintegrations produced by cosmic rays. Proc. Roy. Soc. (London) A 196, 325 - 343, 1949.
  4. Birnbaum, M., Shapiro, M. W., Stiller, B., and O'Dell, F. W., Shape of cosmic-ray star-size distributions in nuclear emulsions. Phys. Rev. 86, 86 - 89, 1952.
  5. Yagoda, H., Behar, A., Davis, R. L., Hewitt, J., and Haymaker, W., Brain study of mice exposed to cosmic rays in the stratosphere and report of nuclear emulsion monitoring in four balloon flights. Military Med. 128, 655 - 672, 1963.
-

TABLE I

Prong Number Distribution of 1,000 Disintegration  
Stars Broken Down into Four Subsets  
of 250 Stars Each

Number of Prongs	Number of Stars Recorded			
	Subset I	Subset II	Subset III	Subset IV
2	61	74	77	58
3	48	43	48	51
4	36	44	31	39
5	31	22	28	30
6	13	14	12	19
7	14	8	11	11
8	6	10	10	7
9	5	7	8	10
10	7	5	4	2
11	8	4	4	7
12	4	1	4	4
13	3	3	1	1
14	2	1	2	2
15	4	5	2	2
16	3	3	3	2
17	2	1	2	3
18	0	2	0	1
19	1	1	0	0
20	1	0	3	1
21	1	1	0	0
22	0	1	0	0

TABLE II

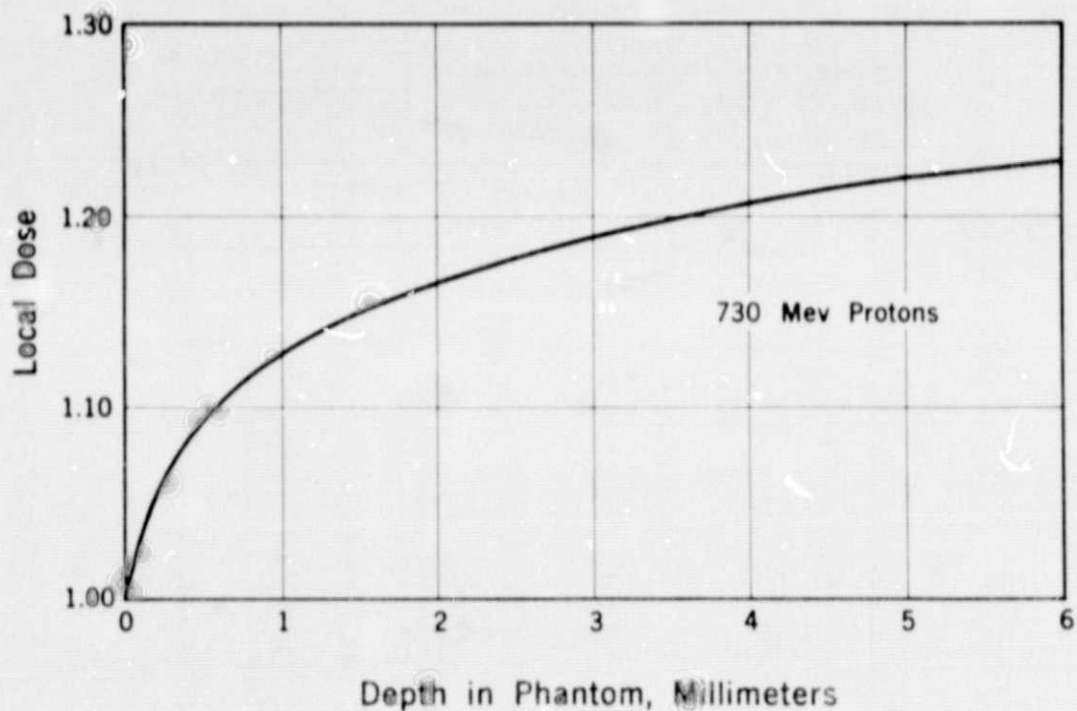
Integral Prong Number Distribution for  
Sets of 250, 500, 750, and 1,000 Disinte-  
gration Stars Assembled from Table I

Minimum Number of Prongs	Integral Number of Stars in Set of			
	250	500	750	1,000
2	250	500	750	1,000
3	189	365	538	730
4	141	274	393	540
5	105	194	288	390
6	74	141	207	279
6	74	141	207	279
7	61	114	168	221
8	47	92	135	177
10	36	64	89	114
12	21	40	57	73

TABLE III

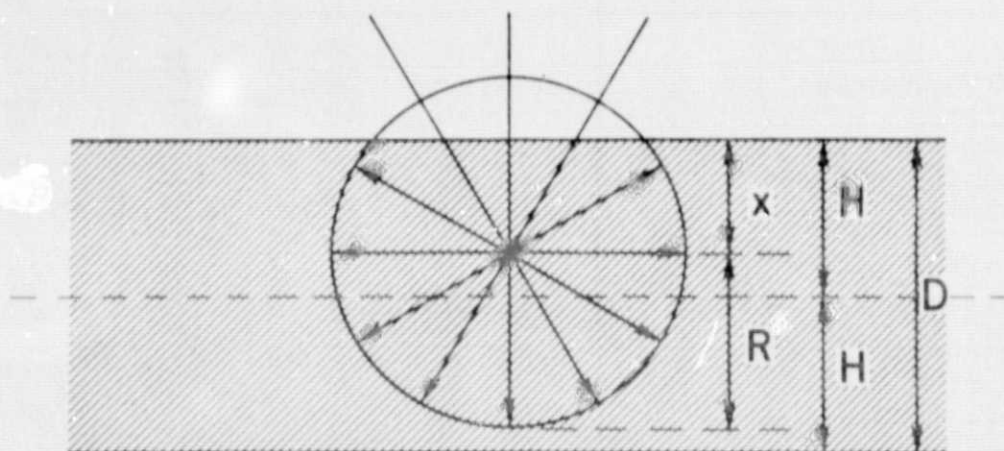
Star Numbers of Best Fit and Standard Deviation  
of Gelatin Star Numbers for Data of Table II

	Number of Stars Recorded			
	250	500	750	1,000
Total Emulsion	254	504	749	1,006
Silverbromide	170	309	462	637
Gelatin	84	195	287	369
Stand. Deviat., Gelatin	20.6	28.5	36.8	40.5
Stand. Deviat., Gelatin, Percent	24.5	14.6	12.1	11.0



BUILD-UP IN POLYSTYRENE PHANTOM  
IRRADIATED WITH 730 MEV PROTONS

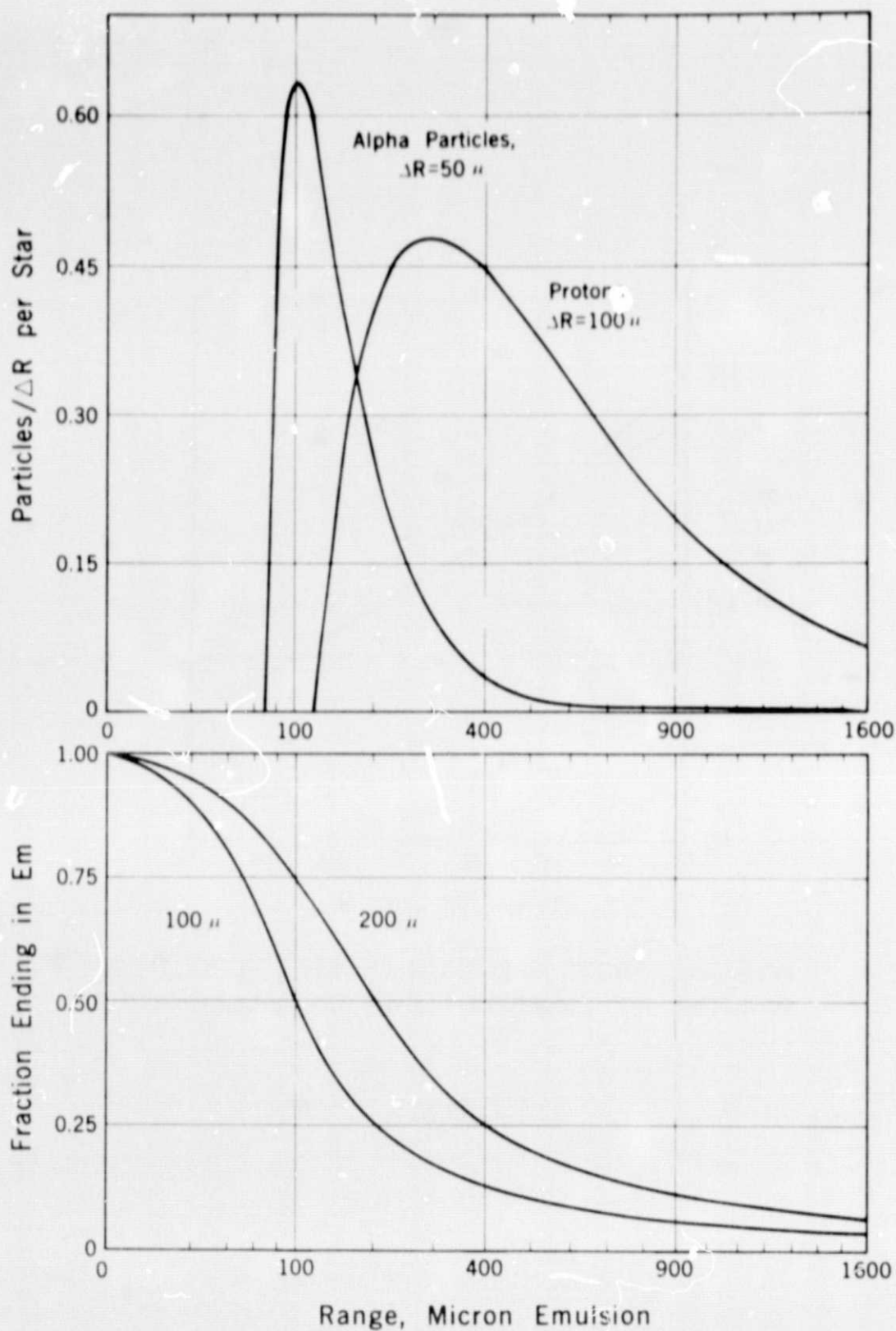
FIGURE 1



BASIC GEOMETRY OF STAR  
PRONGS IN EMULSION LAYER

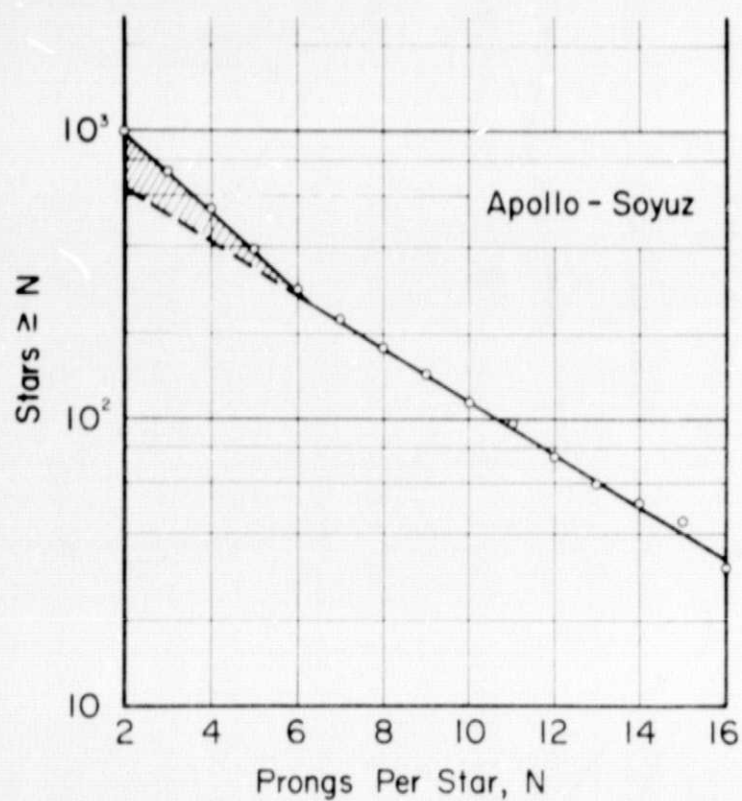
FIGURE 2





DIFFERENTIAL RANGE SPECTRA OF STAR-PRODUCED  
PROTONS AND ALPHA PARTICLES AND RECORDING  
EFFICIENCY OF 100 AND 200  $\mu$  EMULSIONS

FIGURE 3



INTEGRAL PRONG SPECTRUM OF STAR POPULATION  
IN ILFORD K.2 EMULSION FLOWN ON APOLLO-SOYUZ

FIGURE 4